Piecewise parabolic reconstruction methods for free-surface flow

Ronald A. Remmerswaal and Arthur E.P. Veldman*
Bernoulli Institute, University of Groningen, The Netherlands
* Corresponding author: a.e.p.veldman@rug.nl

1 Introduction

The advection of the phase interface plays a central role in the simulation of immiscible, and in our case incompressible, two-phase flow. Explicit modelling of the interface (Tryggvason et al., 2001) results in a highly accurate representation, with the interface resolution essentially unrelated to the resolution of the mesh. The interface can also be represented implicitly, either using a level set or a volume fraction (VoF) function. Using level sets (Osher and Sethian, 1988) results in an efficient method for which changes in topology are automatically taken into account, but they do not inherently conserve mass and require artificial redistancing (Sussman, 1994). On the contrary, VoF methods (see e.g. Hirt and Nichols (1981); Lopez et al. (2004); Puckett et al. (1997); Rider and Kothe (1997); Weymouth and Yue (2010); Youngs (1982)) can inherently conserve mass and result, in particular if geometric VoF methods are considered, in a sharper interface; e.g. Fig. 1(b).

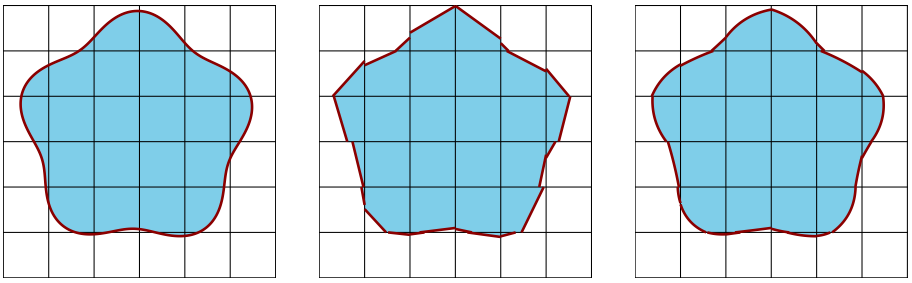

(a) Exact liquid domain. (b) Piecewise linear. (c) Piecewise parabolic.

Fig. 1: Example of a liquid domain and two different approximations (using the MoF and PMoF method respectively).

For capillary driven flow the interface curvature is essential in the modelling of surface tension via the imposition of the Young-Laplace jump condition. When traditional geometric reconstruction methods, that are based on the piecewise linear approximation of the interface (Fig. 1(b)), are used, we find that the curvature from LHFs does not converge under mesh refinement for time-dependent problems. A theoretical understanding is provided in Sects. 2 and 3 where we analyse the accuracy of the advection method and of the LHF based curvature respectively. These results are confirmed numerically in Sect. 5. Based on this observed lack of convergence, we propose to use a piecewise parabolic approximation of the interface instead, as shown in Fig. 1(c) and discussed in Sect. 4.

We denote the time step by δ, and the maximum diameter of all control volumes by h. The numerical approximation $\widetilde{y}(\delta, h)$ converges when $\widetilde{y} \to y$ under mesh refinement while $\delta \leq \frac{h}{U}$ (CFL restriction).

2 Advection methods based on Lagrangian remapping

We denote the computational domain by $\Omega \subset \mathbb{R}^2$, the interface between the two fluids by $I(t)$ and the liquid domain by $\Omega^l(t) \subset \Omega$. The zeroth and first moment of some set $A \subset \mathbb{R}^2$ will be denoted by

$$M_0(A) := \int_A \mathrm{d}V, \quad \mathbf{M}_1(A) := \int_A \mathbf{x}\, \mathrm{d}V,$$

respectively. The liquid volume $M^l_{0,c}$ and its control volume fraction $\chi_c \in [0,1]$ are then defined as

$$M^l_{0,c} := M_0(c \cap \Omega^l), \quad \chi_c(t) := \frac{M^l_{0,c}}{M_0(c)},$$

for some control volume $c \subset \Omega$. The liquid first moment is similarly denoted by $\mathbf{M}^l_{1,c}$.

2.1 Lagrangian remapping

We let $\Psi^\delta \mathbf{x}_0$ denote the flow map of the velocity field $\mathbf{u}$ over the time interval $[t^{(n)}, t^{(n+1)}]$, that is $\Psi^\delta \mathbf{x}(t^{(n)}) = \mathbf{x}(t^{(n+1)})$. The preimage of the control volume c under the flow map, which we denote by $\Psi^{-\delta} c$, is the set of points which ends up inside c; see Fig. 2.

(a) The black curves correspond to the boundary of the preimage of c, which is denoted by $\Psi^{-\delta} c$. The red curve corresponds to the fluid interface $I^{(n)}$ and the shaded region corresponds to $\Psi^{-\delta} c \cap \Omega^{l,(n)}$ (c.f. the right-hand side of Eq. (2)).

(b) The black square corresponds to the boundary of the control volume c. The red curve corresponds to the fluid interface $I^{(n+1)}$ and the shaded region corresponds to $c \cap \Omega^{l,(n+1)}$ (c.f. the left-hand side of Eq. (1)).

Fig. 2: Illustration of a Lagrangian remapping step, see also Eqs. (1) and (2).

The interface $I(t)$ is advected with $\mathbf{u}$, hence $I^{(n+1)} = \Psi^\delta I^{(n)} \Rightarrow \Omega^{l,(n+1)} = \Psi^\delta \Omega^{l,(n)}$. By the invertibility of Ψ^δ we have $\Psi^\delta(A \cap B) = \Psi^\delta A \cap \Psi^\delta B$ and therefore

$$c \cap \Omega^{l,(n+1)} = \Psi^\delta(\Psi^{-\delta} c \cap \Omega^{l,(n)}). \tag{1}$$

Computing the zeroth moment of Eq. (1), and using that $\mathbf{u}$ is divergence free, i.e. the flow map is area preserving $M_0(\Psi^\delta A) = M_0(A)$, results in

$$M_{0,c}^{l,(n+1)} = M_0\left(\Psi^{-\delta} c \cap \Omega^{l,(n)}\right). \tag{2}$$

Equation (2) is key to understanding how a Lagrangian remapping-based geometric VoF method can be constructed, since such a method approximates each of the terms on the right-hand side of Eq. (2):

- The liquid domain $\Omega^{l,(n)}$ is approximated per control volume.
- The preimage $\Psi^{-\delta} c$ is approximated by a polygon whose nodes are approximated using numerical integration. The involved approximation errors will be discussed next.

2.2 Approximate Lagrangian remapping

We denote the exact preimage of the control volume c by $\mathcal{P}_c := \Psi^{-\delta} c$.The approximate preimage $\widetilde{\mathcal{P}_c}$ is constructed by making two approximations. First we approximate the preimage by a polygonal representation denoted by $\mathcal{P}_c^{\text{Rep}}$, which is defined by connecting the corners of the exact preimage $\mathcal{P}_c$ by straight line segments, as is shown in Fig. 3.

Secondly, we approximate the flow map using a numerical integration method. This means we approximately integrate along pathlines, where the velocity field $\mathbf{u}(t, x)$ is now linearly interpolated (in space and time) from a staggered velocity field. For the time integration we use the second-order accurate Heun's method, which, as we will see, is sufficiently accurate for this purpose. This results in the following approximate liquid volume

$$\widetilde{M_{0,c}^l} = M_0\left(\widetilde{P_c} \cap \widetilde{\Omega_c^l}\right). \tag{3}$$

The method described here is very similar to the Lagrangian-Eulerian advection scheme (LEAS) presented in Zinjala and Banerjee (2015).

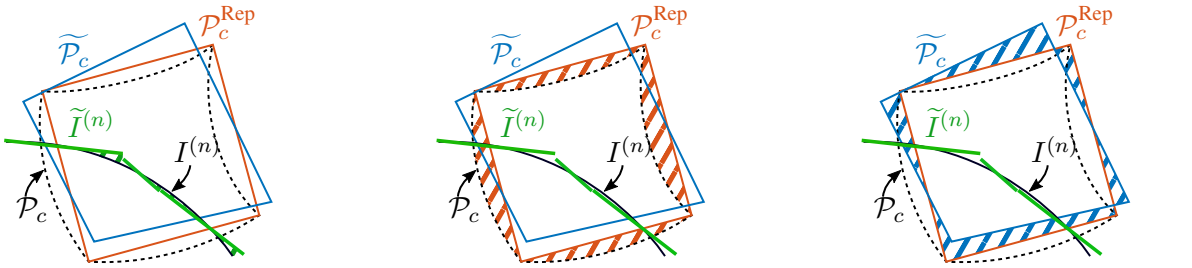

(a) Reconstruction error E_0^{Rec}. (b) Representation error E_0^{Rep}. (c) Integration error E_0^{Int}.

Fig. 3: Illustration of the three error contributions. The dashed black line represents the boundary of the preimage of c, whereas its polygonal approximation $\mathcal{P}_c^{\text{Rep}}$ and fully approximated polygon $\widetilde{\mathcal{P}_c}$ are denoted by the red and blue lines respectively. Furthermore, the interface $I^{(n)}$ at $t = t^{(n)}$ corresponds to the curved black line, whereas the approximate piecewise linear interface $\widetilde{I}^{(n)}$ is represented by the green lines.

We can estimate the error in the volume fractions, due to the two approximations made in the preimage as well as the approximation of the liquid domain. Hereto we use the symmetric difference of two sets $A, B \subset \mathbb{R}^2$ by $A \triangle B := (A \cup B) \setminus (A \cap B)$.We define the following errors, illustrated in Fig. 3:

$$\textit{reconstruction error:} \quad E_0^{\text{Rec}} := M_0\left(\widetilde{\Omega_c^l} \triangle \Omega_c^l\right) = \mathcal{O}(h^r); \tag{4a}$$

$$\textit{representation error:} \quad E_0^{\text{Rep}} := M_0\left(\mathcal{P}_c^{\text{Rep}} \triangle \mathcal{P}_c\right) = \mathcal{O}(h\delta(h+\delta)^2); \tag{4b}$$

$$\textit{integration error:} \quad E_0^{\text{Int}} := M_0\left(\widetilde{\mathcal{P}_c} \triangle \mathcal{P}_c^{\text{Rep}}\right) = \mathcal{O}(h\delta(h+\delta)^2 + h\delta^{q+1}). \tag{4c}$$

Here Ω_c^l denotes the liquid neighbourhood centered around the control volume c $\Omega_c^l = \Omega^l \cap \bigcup_{c' \in \mathcal{C}(c)} c'$, where $\mathcal{C}(c)$ is the set of control volumes which share at least one node with c (i.e. a 3×3 neighbourhood of control volumes if the mesh is rectilinear). Further, r denotes the local order of accuracy of the liquid domain approximation (e.g. $r = 3$ for the MoF method (Dyadechko and Shashkov, 2005)) and q is the order of accuracy of the time integration method. The estimates for these erros have been obtained by studying their constructions in Fig. 3.

Zhang (2013, Eq. 3.15) has shown how the error resulting from a Lagrangian remapping method can be bounded by the above errors:

$$\left|\widetilde{M_{0,c}^l} - M_{0,c}^l\right| \leq E_0^{\text{Rec}} + E_0^{\text{Rep}} + E_0^{\text{Int}}. \tag{5}$$

This then leads to the following consistency result:

Theorem 1 (Consistency of a Lagrangian remapping method) *The following single time step consistency result holds if $\delta \propto h$ (as is the case under a CFL time step restriction)*

$$\|\widetilde{\chi} - \chi\|_{L^\infty} = \underbrace{\mathcal{O}(h^{r-2})}_{\textit{reconstruction}} + \underbrace{\mathcal{O}(h^2)}_{\textit{representation}} + \underbrace{\mathcal{O}(h^2 + h^q)}_{\textit{integration}}.$$

The accuracy of the volume fractions is limited by the reconstruction accuracy whenever a piecewise linear approximation of the interface, for which $r = 3$, is used. An increase of the reconstruction accuracy to $r = 4$, would yield an improvement of the L^∞-error of the volume fractions from first- to second-order accuracy, while using the same Lagrangian remapping method.

3 Curvature

We now turn to the observed lack of curvature convergence in time-dependent problems, as discussed in Sect. 1. The curvature κ is computed for each interface control volume using a LHF resulting from a principal normal direction which is aligned with one of the co-ordinate axes (Gerrits and Veldman, 2003; Popinet, 2009). Given such a LHF, which we denote by $H(y)$, the curvature can be computed as

$$\widetilde{\kappa}_j := \widetilde{H''}(y)\left(1 + \left(\widetilde{H'}(y)\right)^2\right)^{-3/2},$$

where the usual second-order finite difference approximations are applied.

This results in a $(p+1)$-st order accurate approximation to $H(y)$, when the volume fractions are p-th order accurate (so $p = \min(r-2, 2, q)$ according to Thm. 1). Three consecutive values of the LHF are needed for the LHF based approximation of the interface curvature. Whenever this is not possible we combine LHFs from different principal normal directions, as proposed by Popinet (2009), resulting in the generalised height-function (GHF) method.

For the first- and second-order derivatives this implies

$$\widetilde{H_j^{[\lambda]}} = H_j^{[\lambda]} + \mathcal{O}(h^2) + \mathcal{O}(h^{p+1-\lambda}), \quad \lambda = 1, 2.$$

Hence, when a piecewise linear approximation of the interface is used, for which $r = 3$, we find that the volume fractions $\bar{\chi}$ will be first order accurate ($p = \min(r-2, 2, q) = 1$) and thus the approximated second derivative is inconsistent, resulting in a lack of curvature convergence. Convergence of the second derivative of the LHF requires a more accurate liquid domain approximation for which $r \geq 4$ (which results in $p = \min(r-2, 2, q) = 2$); in turn this would then also lead to a convergent curvature. This is our main motivation to introduce piecewise parabolic approximations of the interface as generalisations of the piecewise linear approximations like (E)LVIRA and MoF.

4 Linear and parabolic optimisation-based reconstruction methods

In our piecewise linear and parabolic optimisation-based interface reconstruction methods, the surface approximation is found by minimizing a cost function. All methods considered use (parts of) the two-dimensional search space P_2:

$$P_2 := \{\, p(\mathbf{x}) = \eta^T(\mathbf{x} - \mathbf{x}_c) - s(\eta, \kappa; M_{0,c}^l) + \frac{\kappa}{2}(\tau^T(\mathbf{x} - \mathbf{x}_c))^2 \mid \eta \in S^1, \kappa \in \mathbb{R} \,\}, \tag{6}$$

where $\tau \perp \eta$ is the interface tangent and κ denotes the curvature. consisting of parabolas defined relative to $\mathbf{x}_c$ (the centroid of the control volume c). We denote by P_1 the subspace of P_2 where the curvature $\kappa = 0$, whereas P_2^κ is the subspace where the curvature is known a priori (from the LHF), which reduces the dimensionality of the search space by one. Two cost functionas are considered:

- The (efficient) least squares interface reconstruction algorithm (E)LVIRA (Pilliod and Puckett, 2004; Puckett, 1991) uses the cost function

$$f_{L^2}(p) := \left\{ \sum_{c' \in \mathcal{C}(c)} M_0(c') \left(\frac{M_{0,c'}^l - M_0(c' \cap l\,(p))}{M_0(c')} \right)^2 \right\}^{1/2}, \tag{7}$$

  where $\mathcal{C}(c)$ denotes the set of control volumes which share at least one node with c, while $l\,(p) := \{\mathbf{x} \in \mathbb{R}^2 \,|\, p(\mathbf{x}) \leq 0\}$. In this was, the L^2-norm of the difference between the actual and reconstructed (by extending the interface to c') volume fractions is considered in a neighbourhood around the control volume c.

- The moment of fluid method MoF (Dyadechko and Shashkov, 2005) proposes to include a reference first moment $\mathbf{M}_{1,c}^{l,*}$ for each control volume c to determine the interface normal. Given such a reference first moment, the interface normal is determined by requiring the reconstructed first moment to be as close as possible to this reference first moment. This is achieved via optimisation of the cost function

$$f_{\mathbf{M}_1}(p) := |\mathbf{M}_{1,c}^{l,*} - \mathbf{M}_1(c \cap l\,(p))|_2, \tag{8}$$

  where $|\cdot|_2$ denotes the Euclidean norm. Contrary to other PLIC methods, the MoF method uses only information (the zeroth and first moment) from the control volume itself, resulting in increased accuracy in particular when the interface is only nearly resolved ($\kappa h \approx 1$). Of course, if the reference moments $M_{0,c}^l$ and $\mathbf{M}_{1,c}^{l,*}$ originate from a linear interface, then there must exist a normal angle and thus $p^* \in P_1$ for which $f_{\mathbf{M}_{1,c}}(p^*) = 0$ and hence the MoF method reconstructs linear interfaces exactly.

The parabolic reconstruction of surface tension (PROST) method (Renardy and Renardy, 2002) uses the f_{L^2} cost function and the full P_2 search space. They report reduced spurious currents thanks to a balanced surface tension formulation as well as the accurate curvature obtained from the parabolic reconstruction. We are however quite satisfied with the curvature obtained from the GHF method (Popinet, 2009), and therefore propose to use this curvature in combination with the P_2^κ search space. This method is refered to as the parabolic LVIRA (PLVIRA) method. The same search space P_2^κ has also been used in combination with the MoF cost function $f_{\mathbf{M}_1}$. The resulting method is called PMoF.

5 Results

Reconstruction flower shape We first consider the reconstruction accuracy for a steady problem involving the 'flower shape' as shown in Fig. 1. In Fig. 4 we show the accuracy in terms of the symmetric difference as a function of the grid size. Comparing the results for ELVIRA and PLVIRA, we obtain one additional order of accuracy when using a parabolic reconstrucition versus a linear one. No significant difference in reconstruction accuracy is found between the PROST and PLVIRA methods, confirming that indeed the GHF curvature is sufficiently accurate. A significant increase in accuracy is found for the PMoF method as compared to the PLVIRA method: about one order of magnitude. These results seem to suggest that the interface representation accuracy goes up by one order to $r = 4$, and we are hopeful that the curvature may now also converge for time-dependent problems; see the next test problem.

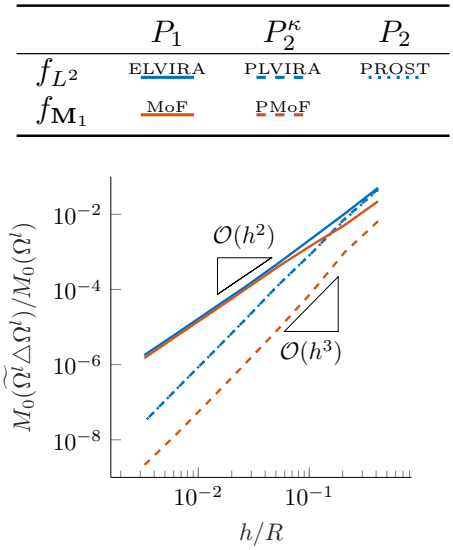

Fig. 4: Reconstruction accuracy of the flower shape, measured in terms of the symmetric difference. Note that the results for PLVIRA and PROST essentially overlap.

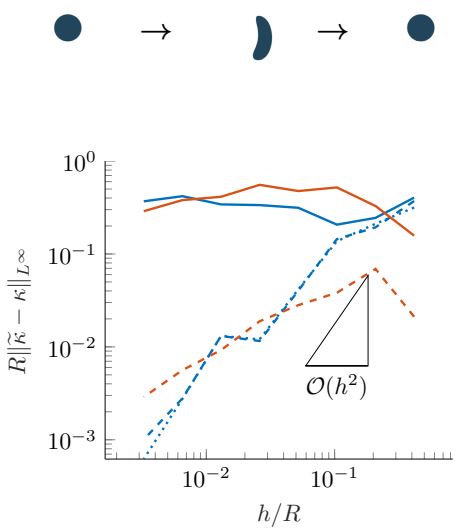

Fig. 5: Accuracy of the interface curvature for the vortex reverse problem at $t = T$. Again the results for PLVIRA and PROST essentially overlap.

Vortex reverse The time-dependent accuracy of the proposed interface advection method is evaluated using the classical vortex reverse problem (Rider and Kothe, 1997) where the interface undergoes a reversible deformation. We find that the PLIC methods do not lead to a convergent curvature, as can be explained from the discussion in Sect. 3. The PMoF method yields a first-order accurate curvature, which we expected from the aforementioned discussion. Interestingly, the PLVIRA and PROST methods even yield a second-order accurate curvature, which we cannot explain from the arguments in Sect. 3.

6 Conclusion

We showed that traditional geometric PLIC linear reconstruction methods do not yield convergence (under mesh refinement) of the curvature for time-dependent advection problems. Therefore, two new geometric VoF interface reconstruction methods are introduced: PLVIRA and PMoF. Both are examples in a class of PPIC methods which are based on a piecewise parabolic approximation of the interface.

The proposed PPIC methods perform favorably when compared to the PLIC methods like (E)LVIRA: the reconstruction accuracy is increased, resulting in a convergent curvature for time-dependent advection problems. For the test cases shown, which featue a prescribed velocity field, the parabolic PROST method is equally accurate. But for a droplet translation problem (not shown in this abstract) where the interface advection method is coupled (via surface tension) to the two-phase Navier–Stokes solver ComFLOW (Kleefsman, 2005; Van der Plas, 2017; Wemmenhove, 2008), we do observe different results for the PLVIRA and PROST methods; only the former behaves as predicted by theory. The work presented in this abstract has been discussed in two spatial dimensions. An extension to 3D is under construction; the extension of the PPIC methods will make use of the second-order zeroth moment calculation of Renardy and Renardy (2002).

Acknowledgements This work is part of the research programme SLING, which is (partly) financed by the Netherlands Organisation for Scientific Research (NWO).

References

Dyadechko, V. and Shashkov, M. (2005). Moment-of-fluid interface reconstruction. *Mathematical Modeling and Analysis*, 836:1–41.

Gerrits, J. and Veldman, A. E. P. (2003). Dynamics of liquid-filled spacecraft. *Journal of Engineering Mathematics*, 45:21–38.

Hirt, C. W. and Nichols, B. D. (1981). Volume of fluid (VOF) method for the dynamics of free boundaries. *Journal of Computational Physics*, 39(1):201–225.

Kleefsman, T. (2005). *Water Impact Loading on Offshore Structures*. PhD thesis, Rijksuniversiteit Groningen.

Lopez, J., Hernandez, J., Gomez, P., and Faura, F. (2004). A volume of fluid method based on multidimensional advection and spline interface reconstruction. 195:718–742.

Osher, S. and Sethian, J. A. (1988). Fronts propagating with curvature-dependent speed: Algorithms based on Hamilton-Jacobi formulations. *Journal of Computational Physics*, 79(1):12–49.

Pilliod, J. E. and Puckett, E. G. (2004). Second-order accurate volume-of-fluid algorithms for tracking material interfaces. *Journal of Computational Physics*, 199(2):465–502.

Popinet, S. (2009). An accurate adaptive solver for surface-tension-driven interfacial flows. *Journal of Computational Physics*, 228(16):5838–5866.

Puckett, E. G. (1991). A volume-of-fluid interface tracking algorithm with applications to computing shock wave refraction. In *Proceedings of the Fourth International Symposium on Computational Fluid Dynamics*, pages 933–938.

Puckett, E. G., Almgren, A. S., Bell, J. B., Marcus, D. L., and Rider, W. J. (1997). A high-order projection method for tracking fluid interfaces in variable density incompressible flows. *Journal of Computational Physics*, 130(2):269–282.

Renardy, Y. and Renardy, M. (2002). PROST: A Parabolic Reconstruction of Surface Tension for the Volume-of-Fluid Method. *Journal of Computational Physics*, 183(2):400–421.

Rider, W. J. and Kothe, D. B. (1997). Reconstructing Volume Tracking. *Journal of Computational Physics*, 141:112–152.

Sussman, M. (1994). A level set approach for computing solutions to incompressible two-phase flow. *Journal of Computational Physics*, 114(1):146–159.

Tryggvason, G., Bunner, B., Esmaeeli, A., Juric, D., Al-Rawahi, N., Tauber, W., Han, J., Nas, S., and Jan, Y. J. (2001). A Front-Tracking Method for the Computations of Multiphase Flow. *Journal of Computational Physics*, 169(2):708–759.

Van der Plas, P. (2017). *Local grid refinement for free-surface flow simulations*. PhD thesis, Rijksuniversiteit Groningen.

Wemmenhove, R. (2008). *Numerical Simulation of Two-Phase Flow in Offshore Environments*. PhD thesis, Rijksuniversiteit Groningen.

Weymouth, G. D. and Yue, D. K. (2010). Conservative Volume-of-Fluid method for free-surface simulations on Cartesian-grids. *Journal of Computational Physics*, 229(8):2853–2865.

Youngs, D. L. (1982). Time-dependent multi-material flow with large fluid distortion. *Numerical Methods in Fluid Dynamics*.

Zhang, Q. (2013). On a family of unsplit advection algorithms for volume-of-fluid methods. *SIAM Journal on Numerical Analysis*, 51(5):2822–2850.

Zinjala, H. K. and Banerjee, J. (2015). A Lagrangian-Eulerian Volume-Tracking with Linearity-Preserving Interface Reconstruction. *Numerical Heat Transfer, Part B*, 68:459–478.